A Density Functional Theory and Electron Momentum Spectroscopy Study into the Complete Valence Electronic Structure of Cubane

W. Adcock,[†] M. J. Brunger,*[,‡] I. E. McCarthy,[†] M. T. Michalewicz,[§] W. von Niessen,[||] F. Wang,[⊥] E. Weigold,[#] and D. A. Winkler[§]

Contribution from the School of Chemistry, Physics and Earth Sciences, Flinders University of South Australia, GPO Box 2100, Adelaide, South Australia 5001, Australia, Institute für Physikalische und Theoretische Chemie, Technische Universität, D-38106, Braunschweig, Germany, School of Chemistry, University of Melbourne, Parkville, Victoria 3052, Australia, Institute of Advanced Studies, Research School of Physical Sciences and Engineering, The Australian National University, Canberra, ACT 0200, Australia, and Division of Molecular Sciences, CSIRO, Private Bag 10, Clayton South MDC, Victoria 3169, Australia

Received November 17, 1999. Revised Manuscript Received February 2, 2000

Abstract: A study of the electronic structure of the complete valence shell of cubane is reported. Results from our many-body Green's function calculation, to the third-order algebraic diagrammatic construction (ADC(3)) level, for the binding energies and spectroscopic factors of the respective valence orbitals of cubane are presented. Binding-energy spectra were measured in the energy regime 6−35 eV over a range of different target electron momenta, so that momentum distributions (MDs) could be determined for each orbital. The corresponding theoretical MDs were calculated using a plane wave impulse approximation (PWIA) model for the reaction mechanism and density functional theory (DFT) for the wave function. Seven basis sets, at the local density approximation (LDA) level and, additionally, incorporating nonlocal correlation functional corrections, were studied. The sensitivity of the level of agreement between the experimental and theoretical MDs to the nonlocal corrections is considered. A critical comparison between the experimental and theoretical MDs allows us to determine the "optimum" wave function for cubane from the basis sets we studied. This wave function is then used to derive cubane's chemically interesting molecular properties. A summary of these results and a comparison of them with those of other workers is presented with the level of agreement typically being good.

Introduction

Since its successful synthesis in 1964 by Eaton and Cole,[1,2] the structure and molecular properties of cubane (C_8H_8) have been studied extensively by both experimental and theoretical chemists and physicists.[3,4] Excellent reviews on the state of our knowledge, with regard to cubane's structural and molecular properties, can be found in Eaton,[3] Yildirim et al.,[5] and Tsanaktsidis.[4] Consequently, only a precis of these results, particularly those related to our discussion in section 5, is presented here.

Cubane belongs to the octahedral point group O_h and has cubic symmetry, although we note that in its crystalline form it is rhombohedral ($a = 5.34$ Å; $\alpha = 72.26°$).[6−8] Consistent with its highly symmetric structure is a notable vapor pressure[3] (1.1 mm at 25 °C) and a significant density[3] of 1.29 g/cm^3. Its recommended[4] C−C and C−H bond lengths of 1.571 and 1.109 Å, respectively, are taken from the work of Hedberg et al.[9] The CCH and CCC bond angles are, however, less precisely known and, respectively, lie in the ranges[10] 123−127° and 89.3−90.5°. Additional properties, such as its strain energy[4] (157.4 kcal/mol) and ^{1}H and ^{13}C NMR spectra,[11,12] have also been reported. In the latter case it was found that cubane produced single resonances at 4.04 ppm[11] and 47.3 ppm,[12] respectively, while the sole ^{1}H−^{13}C−H coupling constant was determined by Della et al.[12] as 153.8 Hz. Finally we note that experimental infrared (IR)[13] and Raman spectroscopy[14] studies into cubane's vibrational modes are available in the literature, as are extensive series of calculations on this same topic (see Miaskiewicz and Smith[15] and references therein).

Contrary to the situation described immediately above for the physicochemical properties of cubane, experimental studies into the valence electronic structure of C_8H_8 have been more

[†] Flinders University of South Australia.
[‡] Present address: Department of Physics and Astronomy, University College London, Gower Street, London WC1E 6BT, U.K.
[§] CSIRO.
[||] Technische Universitat.
[⊥] University of Melbourne.
[#] The Australian National University.

(1) Eaton, P. E.; Cole, T. W., Jr. *J. Am. Chem. Soc.* **1964**, *86*, 962.
(2) Eaton, P. E.; Cole, T. W. Jnr. *J. Am. Chem. Soc.* **1964**, *86*, 3157.
(3) Eaton, P. E. *Angew. Chem., Int. Ed. Engl.* **1992**, *31*, 1421.
(4) Tsanaktsidis, J. *Adv. Strain Org. Chem.* **1997**, *6*, 67.
(5) Yildirim, T.; Gehring, P. M.; Neumann, D. A.; Eaton, P. E.; Emrick, T. *Carbon* **1998**, *36*, 809.
(6) Fleischer, E. *J. Am. Chem. Soc.* **1964**, *86*, 3889.
(7) Yildirim, T.; Gehring, P. M.; Neumann, D. A.; Eaton, P. E.; Emrick, T. *Phys. Rev. Lett.* **1997**, *78*, 4938.
(8) Richardson, S. L.; Matins, J. L. *Phys. Rev. B* **1998**, *58*, 15307.
(9) Hedberg, L.; Hedberg, K.; Eaton, P. E.; Nodari, N.; Robiette, A. G. *J. Am. Chem. Soc.* **1991**, *113*, 1514.
(10) Schubert, W.; Yoshimine, M.; Pacansky, J. *J. Phys. Chem.* **1981**, *85*, 1340.
(11) Edward, J. T.; Farrell, P. G.; Langford, G. E. *J. Am. Chem. Soc.* **1976**, *98*, 3075.
(12) Della, E. W.; Hine, P. T.; Patney, H. K. *J. Org. Chem.* **1977**, *42*, 2940.
(13) Vlahacos, C. P.; Hameka, H. F.; Jensen, J. O. *Chem. Phys. Lett.* **1996**, *259*, 283.
(14) Della, E. W.; McCoy, E. F.; Patney, H. K.; Jones, G. L.; Miller, F. A. *J. Am. Chem. Soc.* **1979**, *101*, 7441.
(15) Miaskiewicz, K.; Smith, D. A. *Chem. Phys. Lett.* **1997**, *270*, 376.

10.1021/ja9940423 CCC: $19.00 © 2000 American Chemical Society
Published on Web 04/07/2000

restricted. To the best of our knowledge they appear to be limited to the photoelectron spectroscopy (PES) studies of Bodor et al.[16] and Bischof et al.[17] and a preliminary report on some aspects of the present electron momentum spectroscopy (EMS) investigation.[18] Of the two PES studies, by far the most detailed was that of Bischof et al.,[17] who reported high-resolution He (Iα) and He (IIα) spectra. Eight of cubane's nine valence states were observed in this work, with assignments of the bands being made on the basis of ab initio STO-3G and MINDO/3 calculations and Koopmans' theorem. In the present study we have not adopted the orbital nomenclature put forward by Bischof et al.[17] Rather we have preferred that used in Schulman et al.,[19] who numbered the symmetry labels within each irreducible representation with reference to the valence-shell orbitals only (i.e., those of carbon 2s and 2p and hydrogen 1s parentage). From a theoretical perspective, calculations into cubane's valence electronic structure are also quite limited. We note the MINDO/1,2 orbital energy results reported in Bodor et al.,[16] the STO-3G and MINDO/3 orbital energy results given in Bischof et al.,[17] the SCF-Xα, STO-3G, MINDO/3, and INDO orbital energy values reported by Schulman et al.,[19] and the SCF−double-ζ (DZ) level orbital energies provided in Almlöf and Jonvik.[20] It is apparent, however, that there are currently no sophisticated Green's function level calculations for cubane's orbital energies and spectroscopic factors[21] (pole strengths) available in the literature.

EMS, or (e,2e) coincidence spectroscopy, is now a well-developed tool for the investigation of the valence electronic structure of molecules due to its unique ability to measure the orbital momentum profile for binding-energy-selected electrons.[21] Furthermore, within the plane wave impulse approximation (PWIA) and, in many cases, the target Hartree−Fock (THFA) or target Kohn−Sham (TKSA) approximations,[22−24] this measured momentum cross section may be directly compared with the calculated spherically averaged momentum distribution (MD) of a specific molecular orbital, once the appropriate angular resolution function has been folded in.[25] Hence, EMS is also a powerful technique for evaluating the quality of theoretical wave functions in quantum chemistry,[22,26] and in this paper we report its application to cubane. In section 2 we briefly discuss some of the experimental aspects of the EMS technique used in our work, while in section 3 details of our structure calculations are presented. In addition, details of our Green's function calculation, to third order, in the algebraic diagrammatic construction (ADC(3)) method[27] for cubane's orbital energies and spectroscopic factors are also given in this section. The results of the experimental and theoretical MDs are presented and discussed in detail in section 4. The significance of the present application of the EMS technique to this molecule is that by comparing the experimental and theoretical MDs, for the relevant valence orbitals, we can independently determine which of the DFT basis sets we have studied provides the most physically reasonable representation of the cubane molecule. Standard UniChem[28,29] features then allow us to utilize this "optimum" wave function to extract the chemically important molecular property information for the cubane system including bond lengths, bond angles, infrared spectra, and so on. A selection of these data, along with a comparison of them with previous work, is given and discussed in section 5 of this paper. Finally, in section 6, conclusions from the results of the present study are drawn.

2. Experimental Details

The complete valence region of cubane was studied in several experimental runs using the Flinders symmetric noncoplanar electron momentum spectroscopy spectrometer.[21,22] A full description of the coincidence spectrometer and the method of taking the data can be found in McCarthy and Weigold,[21] although we note that since their report there have been three major developments to this apparatus. Specifically, the computer hardware and operating system have been upgraded, the collision region is now differentially pumped, and, finally, an electron monochromator (for the incident electrons) has been brought on-line, an advance that has improved by a factor of about 2 the achievable coincidence energy resolution. A full discussion of these developments is not strictly relevant to this paper and can be found elsewhere.[30]

The high-purity cubane is admitted into the target chamber through a capillary tube, the flow rate being controlled by a variable leak valve. Note that the cubane driving pressure was too low to cause any significant clustering by supersonic expansion. The collision region is surrounded by a chamber pumped by a 700 L s^{-1} diffusion pump. Apertures and slits are cut in the collision chamber for the incident beam and ejected electrons. The differentially pumped collision region makes it possible to increase the target gas density by a factor of about 3 while keeping the background pressure in the spectrometer below 10^{-5} Torr. This was important as it enabled us to maintain workable coincidence count rate levels, even with the smaller electron beam current output from the (e,2e) monochromator (typically 30 μA) compared to that of a normal electron gun.[21] The coincident energy resolution of the present measurements was typically 0.6 eV (fwhm), as determined from measurements of the binding-energy (ϵ_f) spectrum of helium. However, due to the natural line widths of the various transitions (ranging from 0.56 to 1.89 eV), as estimated from the relevant PES spectrum,[17] the fitted resolutions of the spectral peaks for cubane varied from 0.82 to 1.98 eV (fwhm). Nonetheless with the specified improvement in our coincident energy resolution (from ∼1.2 to 0.6 eV), we are now able to deconvolute with confidence the coincidence signal originating from the respective $1e_g$ and $2t_{1u}$ orbitals, and also deconvolve with confidence the coincidence signal originating from the respective $2a_{1g}$ and $1t_{2g}$ orbitals. This would not have been possible without the development of the (e,2e) monochromator.[30] The angular resolution was typically 1.2° (fwhm), as determined from the electron optics and apertures and from a consideration of the argon 3p angular correlation.

In the current study noncoplanar symmetric kinematics was employed, that is, the outgoing electron energies E_A and E_B

(16) Bodor, N.; Dewar, M. J. S.; Worley, S. D. *J. Am. Chem. Soc.* **1970**, *92*, 19.
(17) Bischof, P.; Eaton, P. E.; Gleiter, R.; Heilbronner, E.; Jones, T. B.; Musso, H.; Schmelzer, A.; Stober, R. *Helv. Chim. Acta* **1978**, *61*, 547.
(18) Adcock, W.; Brunger, M. J.; Michalewicz, M. T.; Winkler, D. A. *Aust. J. Phys.* **1998**, *51*, 707.
(19) Schulman, J. M.; Fischer, C. R.; Solomon, P.; Venanzi, T. J. *J. Am. Chem. Soc.* **1978**, *100*, 2949.
(20) Almlöf, J.; Jonvik, T. *Chem. Phys. Lett.* **1982**, *92*, 267.
(21) McCarthy, I. E.; Weigold, E. *Rep. Prog. Phys.* **1991**, *54*, 789.
(22) McCarthy, I. E.; Weigold, E. *Rep. Prog. Phys.* **1988**, *51*, 299.
(23) Coplan, M. A.; Moore, J. H.; Doering, J. P. *Rev. Mod. Phys.* **1994**, *66*, 985.
(24) Casida, M. *Phys. Rev. A* **1995**, *51*, 2005.
(25) Frost, L.; Weigold, E. *J. Phys. B* **1982**, *15*, 2531.
(26) Zheng, Y.; Neville, J. J.; Brion, C. E. *Science* **1995**, *270*, 786.
(27) von Niessen, W.; Schirmer, J.; Cederbaum, L. S. *Comput. Phys. Rep.* **1984**, *1*, 59.
(28) Andzelm, J.; Wimmer, E. *J. Chem. Phys.* **1992**, *96*, 1290.
(29) Komornicki, A.; Fitzgerald, G. J. *J. Chem. Phys.* **1993**, *98*, 1398.
(30) Hewitt, G. B.; Cottrell, G.; Northeast, R.; Utteridge, S.; Brunger, M. J. *Meas. Sci. Technol.* in preparation.

are equal, the two emitted electrons making equal polar angles $\theta = 45°$ with respect to the direction of the incident electrons. The total energy (E), $E = E_0 - \epsilon_f = E_A + E_B$, was 1000 eV. The binding-energy range of interest ($\epsilon_f = 6-35$ eV for cubane) is stepped through sequentially at each of a chosen set of angles ϕ using a binning mode[21] through the entire set of azimuthal angles ($\phi = 0-25°$). Scanning through a range of ϕ is equivalent to sampling different target electron momenta **p** as

$$p = \left[(2p_A \cos\theta - p_0)^2 + 4p_A^2 \sin^2\theta \sin^2\left(\frac{1}{2}\phi\right)\right]^{1/2} \quad (1)$$

For zero binding energy ($\epsilon_f = 0$ eV), $\phi = 0°$ corresponds to $p = 0$ au, and for the present binding energies, angular resolution, and kinematics, $\phi = 0°$ corresponds to $p \sim 0.09$ au. Similarly for $\phi = 10°$, p $\sim$ 0.75 a.u.

Typical binding-energy spectra for cubane are given in Figure 1a,b. The solid curve in each panel represents the envelope of the 15 fitted Gaussians (various dashed curves) whose positions below $\epsilon_f = 22.1$ eV are taken from the available high-resolution PES data.[17] It is clear from these figures that the fits to the measured binding-energy spectra are excellent. The least-squares-fit deconvolution technique used in the analysis of these spectra is based on the work of Bevington and Robinson,[31] to whom interested readers are referred for more detail. Above $\epsilon_f = 22.1$ eV, for the inner valence $1t_{1u}$ and $1a_{1g}$ orbitals, there are no PES data available to aid us in our fitting of the binding-energy spectra. Under these circumstances the positions and widths of the Gaussian peaks, and the number of Gaussians, used in the spectral deconvolution were simply determined by their utility in best fitting the observed data for all ϕ. The fact that the inner valence $1t_{1g}$ orbital needed 2 Gaussians and the innermost valence $1a_{1g}$ orbital needed 5 Gaussians, to incorporate the measured coincidence intensity into the fit, is possibly indicative of the existence of final state correlation effects in the inner valence region of cubane. Alternatively, such an observation is also consistent with the natural line profiles for these orbitals being highly asymmetric. This point is considered again in the next section.

A sample of high-purity cubane ($\sim$1.3 g) was obtained using the procedure of Eaton et al.[32] However, to obtain respectable yields ($\sim$45$-$50%) we found it necessary to change the reported workup procedure. The modifications were as follows. First, the final pentane extract was washed three times with commercial bleach and two times with concentrated hydrochloric acid in order to completely remove unreacted *tert*-butylthiol and the byproduct from the decomposition of the Barton ester, respectively. Second, rather than crystallization of the cubane from pentane by the addition of methanol, the pentane was carefully evaporated in vacuo (90 mm at room temperature) to afford a crude product which was sublimed and collected in a cold trap (acetone/liquid nitrogen). The crude cubane was recrystallized from methanol, collected by filtration, and dried (50 mm at room temperature) with appropriate care.[32] The product was found to be homogeneous with respect to vapor phase chromatographic (vpc) analysis. In addition, if we were to compare our $\phi = 0° + 10°$ binding-energy spectrum with the PES result of Bishof et al.,[17] then it would be apparent that the level of qualitative agreement between them is very good. This is further evidence for the purity of the present cubane sample.

(31) Bevington, P. R.; Robinson, D. K. *Data Reduction and Error Analysis for the Physical Sciences*; McGraw-Hill Inc.: New York, 1990.

(32) Eaton, P. E.; Nordari, N.; Tsansktsidis, J.; Upadhyaya, S. P. *Synthesis* **1995**, 501.

3. Theoretical Analysis

The PWIA is used to analyze the measured cross sections for high-momentum transfer (e,2e) collisions. Using the Born$-$Oppenheimer approximation for the target and ion wave functions, the EMS differential cross section σ, for randomly oriented molecules and unresolved rotational and vibrational states, is given by

$$\sigma = K\int d\Omega |\langle p\Psi_f^{N-1}|\Psi_i^N\rangle|^2 \quad (2)$$

where K is a kinematical factor which is essentially constant in the present experimental arrangement, Ψ_f^{N-1} and Ψ_i^N are the electronic many-body wave functions for the final [$(N-1)$ electron] ion and target [N electron] ground states, and p is the momentum of the electron at the instant of ionization. The $\int d\Omega$ denotes an integral over all angles (spherical averaging) due to averaging over all initial rotational states. The average over the initial vibrational state is well approximated by evaluating orbitals at the equilibrium geometry of the molecule. Final rotational and vibrational states are eliminated by closure.

The momentum space target-ion overlap $\langle p\Psi_f^{N-1}|\Psi_i^N\rangle$ can be evaluated using configuration interaction (CI) descriptions of the many-body wave functions,[24] but usually the weak-coupling approximation[21] is made. Here, the target-ion overlap is replaced by the relevant orbital of, typically, the Hartree$-$Fock or Kohn$-$Sham[33] ground state Φ_0, multiplied by a spectroscopic amplitude. With these approximations, eq 2 reduces to

$$\sigma = KS_j^{(f)}\int d\Omega |\phi_j(p)|^2 \quad (3)$$

where $\phi_j(p)$ is the momentum space orbital. The spectroscopic factor $S_j^{(f)}$ is the square of the spectroscopic amplitude for orbital j and ion state f. It satisfies the sum rule

$$\sum_f S_j^{(f)} = 1 \quad (4)$$

Hence it may be considered as the probability of finding the one-hole configuration in the many-body wave function of the ion.

The present Green's function based calculations on cubane were performed on the experimental structure[6] using the program system MOLCAS2.[34] The basis set employed in this work derives from the atomic natural orbital (ANO) basis of Widmark et al.[35] For the carbon atoms it is (14s,9p,4d)/[4s,2p,1d], and for the hydrogen atoms it is (8s,4p)/[2s,1p]. The present ADC(3) results, calculated using the method of Schirmer et al.,[36] for the binding energies and spectroscopic factors of cubane are given in Table 1 along with the present EMS and corresponding PES results[16,17] for the orbital energies, and the respective orbital binding energies as calculated from the present DFT-BP/TZVP (see below for an explanation of this acronym) and ANO wave functions. There are two points we highlight from the results in this table. First, the current ADC(3) results for ϵ_f, of each respective orbital, are in quite good accord with those correspondingly found in the PES work of Bischof et al.,[18]

(33) Kohn, W.; Sham, L. *J. Phys. Rev.* **1965**, 140, A1133.

(34) Andersson, K.; Blomberg, M. R. A.; Fuelscher, M. P.; Kellö, V.; Lindh, R.; Malmqvist, P.-Å.; Noga, J.; Olsen, J.; Roos, B. A.; Sadlej, A. J.; Siegbahn, P. E. M.; Urban, M.; Widmark, P.-O. *MOLCAS-2*, University of Lund: Lund, Sweden, 1991.

(35) Widmark, P.-O.; Malmqvist, P-Å.; Roos, B. O. *Theor. Chim. Acta* **1990**, *77*, 291.

(36) Schirmer, J.; Cederbaum, L. S.; Walter, O. *Phys. Rev. A* **1983**, *28*, 1237.

Table 1. Cubane Binding Energies (eV) and Spectroscopic Factors (between parentheses)[a]

		exptl			theor		
valence state	orbital nomen	PES[16]	PES[17]	present EMS	present DFT	present ADC(3)	present SCF
1	$2t_{2g}$	8.74	9.6	9.6	6.23	9.56 (0.91)	10.49
2	$1t_{2u}$	8.74	9.6	9.6	6.70	9.91 (0.90)	10.63
3	$1e_g$	13.62	13.7	13.7	10.31	14.44 (0.89)	15.75
4	$2t_{1u}$	13.62	14.3	14.3	10.72	14.58 (0.88)	15.86
5	$1a_{2u}$	15.34	15.6	15.6	11.16	15.81 (0.87)	17.56
6	$2a_{1g}$	16.87	17.6	17.6	13.09	17.61 (0.84)	19.38
						20.27 (0.02)	
7	$1t_{2g}$	17.26	18.5	18.5	13.54	18.48 (0.76)	20.94
						19.84 (0.02)	
8	$1t_{1u}$		22.1	22.1	17.74	21.75 (0.02)	26.61
				22.9		22.21 (0.04)	
						22.74 (0.02)	
						22.84 (0.27)	
						22.99 (0.02)	
						23.28 (0.15)	
						23.37 (0.07)	
						23.95 (0.03)	
9	$1a_{1g}$			27.4	23.37	28.32 (0.07)	33.83
				28.3		29.09 (0.03)	
				29.1		29.27 (0.02)	
				30.3		30.17 (0.04)	
				31.6		30.37 (0.10)	
				32.1		30.74 (0.03)	
						30.83 (0.03)	
						30.95 (0.09)	
						31.66 (0.06)	
						31.75 (0.05)	
						32.47 (0.03)	
						33.03 (0.02)	

[a] Only calculated pole strengths >0.02 are shown in the table. Present DFT, ADC(3), and SCF denote the results of the present calculations, as explained in the text. PES denotes the experimental photoelectron spectroscopy data while present EMS denotes the current experimental results

particularly for the outer valence orbitals. Second, our ADC(3) results predict that the spectroscopic strength of the inner valence $1t_{1u}$ and $1a_{1g}$ orbitals will be severely split due to final state electron correlation effects. This observation is entirely consistent with what we found in the measured EMS binding-energy spectra of Figure 1a,b for $\epsilon_f \geq 20$ eV.

The Kohn−Sham equation[33] of DFT may be considered as an approximate quasiparticle equation, with the potential operator approximated by the exchange-correlation potential.[24] Usually this is done at the local density approximation (LDA) level, although in this study we also employ nonlocal correlation functional corrections. In order to compute the coordinate space Kohn−Sham orbitals ψ_j, we employed DGauss, a program package developed by CRAY Research by Andzelm and colleagues.[28,29] Note that our rationale for using DFT/DGauss over other available packages such as HF/GAUSSIAN has been considered elsewhere,[37] and so we do not repeat those details again here. DGauss is itself a part of UniChem, a suite of computatational quantum-chemistry programs from Oxford Molecular. Using DGauss and UniChem, we employed various basis sets to build a model cubane molecule and then we minimized the energy. The molecular coordinates at the optimum geometry (minimum energy) and the Gaussian molecular orbital parameters (coefficients and exponents) were next treated as input to the Flinders-developed program AMOLD,[21] which computes the momentum space spherically averaged molecular-structure factor[22] and the (e,2e) cross section or momentum distribution.

The comparisons of calculated momentum profiles with experiment (see section 4) may be viewed as an exceptionally detailed test of the quality of the basis set. In this investigation, we have used seven basis sets in the DFT computations. These basis sets are denoted by the acronyms DZ94, DZ94P, DZVP, DZVP2, TZ94, TZ94P, and TZVP. The notations DZ and TZ denote basis sets of double- or triple-ζ quality. *V* denotes a calculation in which such a basis is used only for the valence orbitals and a minimal basis is used for the less chemically reactive core orbitals. The inclusion of long-range polarization functions is denoted by P.

An, in principle, improvement over the LDA approach to approximating the exchange-correlation functional can be obtained by using functionals that depend on the gradient of the charge density (Becke,[38,39] Perdew,[40] and Lee et al.[41]). In this work we employed two different approximations to the exchange-correlation energy functional due to Becke and Perdew (basis sets marked with BP) and Becke, Lee, Yang, and Parr (basis sets marked with BLYP). The nonlocal density-gradient corrections for the aforementioned two nonlocal models, as implemented in DGauss, were included self-consistently throughout the entire computations.

4. Comparison between Experimental and Theoretical Momentum Distributions

Typical binding-energy spectra of C_8H_8 in the region 6−35 eV and at $E = 1000$ eV are given in Figure 1. These spectra were measured at each of a chosen set of angles ϕ and then analyzed with a least-squares-fit deconvolution technique.[31] This analysis then allowed us to derive the required momentum

(37) Michalewicz, M. T.; Brunger, M. J.; McCarthy, I. E.; Norling, V. M. In *CRAY Users Group 1995 Fall Proceedings*; Shaginaw, R., Ed.; 1995; pp 37−41.

(38) Becke, A. D. *Phys. Rev. A* **1988**, *38*, 3098.
(39) Becke, A. D. *J. Chem. Phys.* **1988**, *88*, 2547.
(40) Perdew, J. P. *Phys. Rev. B* **1986**, *33*, 8822.
(41) Lee, C.; Parr, R. G.; Yang, W. *Phys. Rev. B* **1988**, *37*, 785.

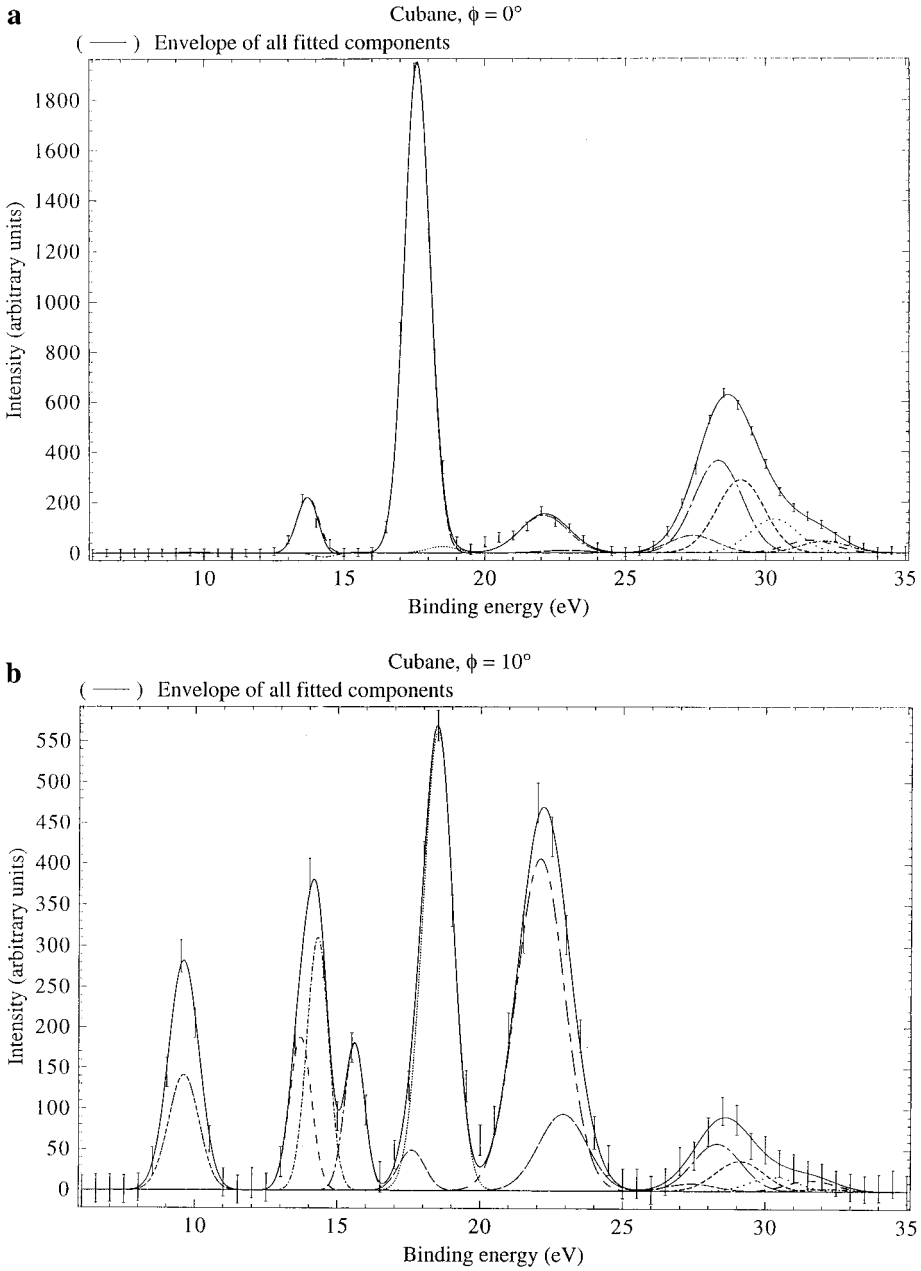

Figure 1. Typical binding-energy spectra from our 1000 eV noncoplanar symmetric EMS investigation into cubane. The curves show the fits to the spectra at (a) $\phi = 0°$ ($p \sim 0.09$ au) and (b) $\phi = 10°$ ($p \sim 0.75$ au) using the known energy resolution.

distributions for all the respective valence orbitals of cubane. Although the measured MDs are not absolute, relative magnitudes for the different transitions are obtained.[21] In the current EMS investigation of the valence states of C_8H_8, the experimental momentum distributions are placed on an absolute scale by summing the experimental flux for each measured ϕ (or, as we saw from eq 1, p) for the first five ($2t_{2g}$, $1t_{2u}$, $1e_g$, $2t_{1u}$, and $1a_{2u}$) outer valence orbitals, and then normalizing this to the corresponding sum from the results of our PWIA DFT-LDA/TZVP calculation.

In Figure 2a we compare our experimental MD for the degenerate highest-occupied molecular orbitals (HOMOs), $2t_{2g} + 1t_{2u}$ at $\epsilon_f = 9.6$ eV, of C_8H_8 with the results from our PWIA DFT-LDA calculations for each of the seven DFT basis states we have considered. We note that the errors on all the present experimental momentum distributions, as derived during the deconvolution procedure, are 1 standard deviation uncertainties.[31] It is clear from Figure 2a that the TZ94P basis functions provide totally inadequate representations of the $2t_{2g} + 1t_{2u}$ orbitals, particularly for momenta $\phi < 12°$. Specifically, TZ94P leads to an initial peak in the MD, at around $\phi = 8°$, that is not seen experimentally or in the other PWIA DFT-LDA calculations. A somewhat unexpected feature, compared to our usual[21] experience, is that these "p-like" $2t_{2g}$ and $1t_{2u}$ outer valence orbitals have a peak in the MD at a remarkably high value of ϕ and have virtually no intensity (see also Figure 1a) at $\phi = 0°$. This very interesting extreme "p-like" behavior of the $2t_{2g} + 1t_{2u}$ orbitals may also point to interesting hybridization. Traditionally, strained cyclic molecules are seen as having "normal" sp^3-hybridized carbons, and the unusual carbon skeleton bond angles are explained by assuming that the sp^3 hybrid orbitals are "bent". The present results suggest that the HOMOs are almost pure "p-like" in character and so are better explained by an sp^n hybrid where n is large. This makes intuitive sense as the three p orbitals on carbon are orthogonal, just like the skeletal carbon bonds. Thus perhaps cubane has C−C bonds

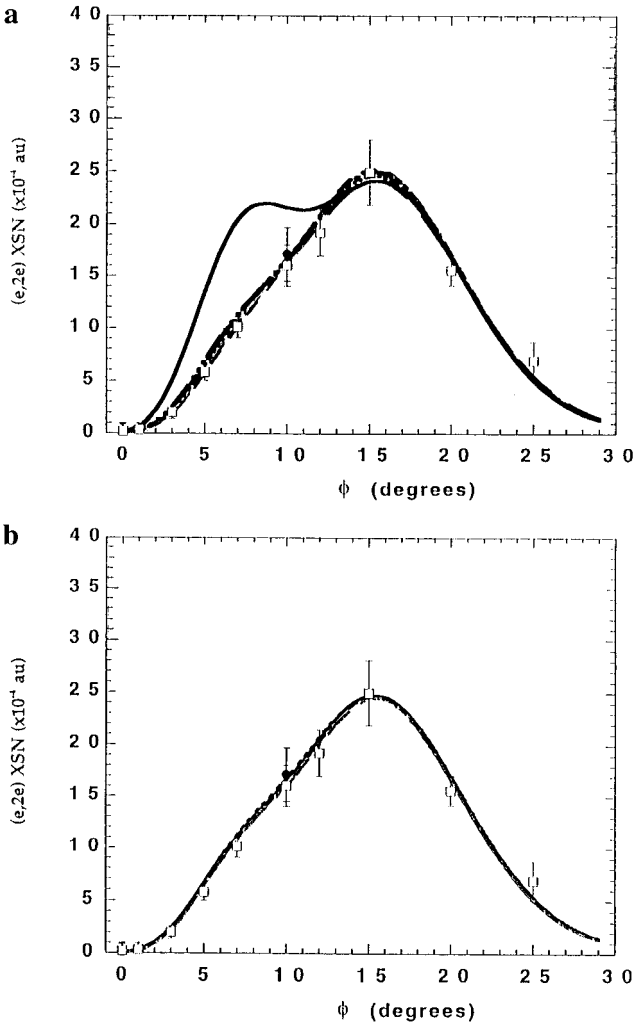

Figure 2. (a) The 1000 eV symmetric noncoplanar momentum distribution for the $2t_{2g} + 1t_{2u}$ HOMOs of cubane. The present data for runs A (●) and B (□) are compared against the results of our PWIA DFT-LDA calculations: (− -) DZ94, (− − −) DZ94P, (- - -) DZVP, (− - -) DZVP2, (− - - - −) TZ94, (—) TZ94P and (- - -) TZVP. (b) The 1000 eV symmetric noncoplanar momentum distribution for the $2t_{2g} + 1t_{2u}$ HOMOs of cubane. The present data for runs A (●) and B (□) are compared against the results of our PWIA DFT-TZVP calculations at the LDA level (- - -), BLYP level (—) and BP level (− - -).

which are formed essentially by σ overlap of "pure" p orbitals. The s orbitals would then go mainly to forming C−H bonds. Theoretical studies of cubane by Schulman and co-workers[19] are consistent with this chemically intuitive approach and provide a rationale for the extremely "p-like" MD observed for the HOMOs. They found that, because of its high symmetry, cubane represents an unusual case of a molecule which has a molecular orbital which is either solely C−C bonding or solely C−H bonding. In a minimal basis set treatment the outer valence $1e_g$ and $1t_{2u}$ (HOMO) orbitals are symmetry determined combinations of 2p orbitals with no 2s admixture. The $2t_{2g}$ (HOMO) orbital is a mixture of C−C and C−H bonds with C−C dominating. Finally, we note that the results in Figure 2a suggest that the experimental EMS spectroscopic factors for both the respective $2t_{2g}$ and $1t_{2u}$ orbitals are ∼1. This observation is entirely consistent with our ADC(3) spectroscopic factor calculations for these orbitals (see Table 1). Figure 2b shows that the PWIA DFT MD result with TZVP basis functions is largely insensitive to whether LDA or BP and BLYP nonlocal functional corrections are used. This observation also holds for

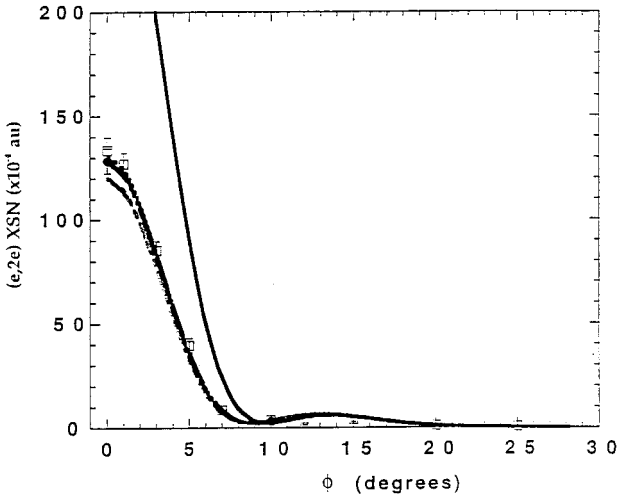

Figure 3. The 1000 eV symmetric noncoplanar momentum distribution for the $2a_{1g}$ orbital of cubane. The legend is the same as that for Figure 2a.

each of the other six DFT basis functions we employed in this study, although for the sake of clarity they are not illustrated here. In addition, this insensitivity of the calculated MDs to whether LDA or BP and BLYP levels are employed is also found to occur for the remaining outer valence ($1e_g$, $2t_{1u}$, and $1a_{2u}$) orbitals, and so we do not illustrate the BP and BLYP results for them in the ensuing discussion. Finally, we note from Figure 2b the excellent agreement between the PWIA DFT-LDA, BP, BLYP/TZVP momentum distribution results and the experimental MD result over all measured ϕ.

In Figure 3 we compare our experimental momentum distribution for the first of the inner valence orbitals, the $2a_{1g}$ orbital at $\epsilon_f = 17.6$ eV, with the results from our PWIA DFT-LDA calculations for each of the seven DFT basis states we have studied. Unlike those for the outermost valence orbitals we previously considered, the $2a_{1g}$ momentum distribution is clearly "s-like" in nature, having a strong maximum in the cross section at $\phi = 0°$. We note, however, the broad secondary peak in this cross section with a much weaker maximum near $\phi = 13.5°$, indicating some "p-like" contribution to the MD for the $2a_{1g}$ orbital. It is apparent from Figure 3 that the PWIA momentum distributions for both the DFT-LDA/DZVP and DZVP2 basis states somewhat underestimate the magnitude of the experimental MD for $\phi < 5°$. In addition, the failure of the DFT-LDA/TZ94P basis to provide an adequate representation for the orbital in question is manifest, particularly for $\phi < 10°$ where the calculated cross section is often a factor of 2.5 times larger than that observed experimentally.

Finally, in Figure 4 we present our experimental and theoretical MDs for the innermost valence $1a_{1g}$ orbital of cubane. In this case the PWIA calculation with the DFT-LDA/DZ94 basis is seen to slightly underestimate the magnitude of the (e,2e) cross section for momenta $\phi < 3°$. The result with the DFT-LDA/DZ94P basis overestimates the magnitude of the $1a_{1g}$ momentum distribution for $\phi < 10°$, while when the DFT-LDA/TZ94P basis is employed, the resulting PWIA MD significantly underestimates the magnitude of the cross section for $\phi < 7°$. Although it is not all that well illustrated in Figure 4, in fact all the theoretical MDs underestimate the strength of the $1a_{1g}$ cross section for $\phi > 15°$. We do not believe this observation is indicative of a general limitation in the DFT basis sets we have considered for the $1a_{1g}$ orbital. Rather, Brunger et al.[42] found in their EMS study of the 4d states of xenon that for tightly bound systems, i.e., inner valence and core states, plane wave

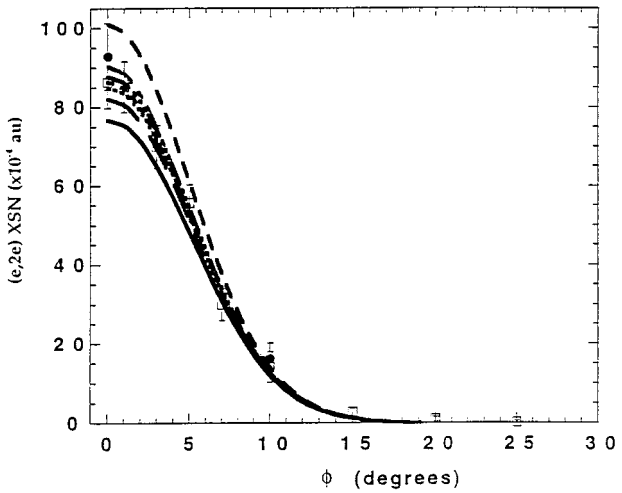

Figure 4. The 1000 eV symmetric noncoplanar momentum distribution for the $1a_{1g}$ innermost valence orbital of cubane. The legend is the same as that for Figure 2a.

approximation calculations might be inadequate and that multicentered distorted wave calculations may be necessary to correctly describe the reaction mechanism. As such multicenter calculations are unavailable for molecules, we can only speculate that this is the true reason for the discrepancy between our $1a_{1g}$ experimental and theoretical MDs for $\phi > 15°$.

The descriptions we provided above, in our comparison of the experimental and theoretical MDs, for a small but representative subset of the valence orbitals of cubane, holds equally well for the remaining $1e_g$, $2t_{1u}$, $1a_{2u}$, $1t_{2g}$, and $1t_{2u}$ orbitals (see Supporting Information). Consequently we do not specifically discuss our MD results for these latter valence orbitals except to highlight two further points. First, the experimental spectroscopic factors for the respective $1e_g$, $2t_{1u}$, and $1a_{2u}$ outer valence orbitals are all found to be ~1, in good accord with our corresponding ADC(3) calculation results (see Table 1). Second, for the $1t_{2g}$ and $1t_{1u}$ orbitals we notice a suggestion that the PWIA calculation with the DFT-TZVP/BP basis and nonlocal correction provides a somewhat better description of the experimental MD than does either of the corresponding TZVP/LDA or TZVP/BLYP results (see Supporting Information).

If we now briefly summarize the results embodied in Figures 2−4, and the additional figures in our Supporting Information, we note that there is little to separate the quality of the description of the experimental MDs, for all the valence orbitals, provided by both the PWIA DFT-LDA/TZVP and DFT-LDA/TZ94 calculations. After very careful consideration of our results, we conclude that of these two basis sets the PWIA DFT-LDA/TZVP calculation provides a marginally superior description of the experimental results. In addition, the total energy of the present DFT-BLYP/TZVP wave function was −309.4009 E_h, while that for the present DFT-BLYP/TZ94 wave function was −309.3138 E_h. As the total energy of the TZVP result is lower (more negative) than that of the TZ94 result, we can surmise that it provides the most stable configuration for the cubane molecule for the basis states considered. Consequently when we couple this latter result with that afforded by our comprehensive comparison between the experimental and theoretical MDs, we conclude that our "optimum" wave function for the cubane molecule is DFT-TZVP.

Table 2. Bond Lengths in Cubane Calculated in This Work, Compared with Other Experimentally Determined Geometries

methods	r_e (C−C) Å	r_e (C−H) Å
DFT/TZVP (present)	1.575	1.098
electron diffraction[49]	1.571	1.098
microwave spectroscopy[50]	1.5708	1.097
X-ray diffraction[6]	1.551	1.040

5. Molecular Property Information

Experimental validation of Hartree−Fock or density functional basis sets using EMS may provide a route to appropriate basis sets for calculating other types of molecular properties, such as molecular geometries, charge distributions, and orbital energies. Previous work[13,15,17,43−48] has used a variety of molecular orbital (MO) approaches to determine structural and electronic properties of cubane. We took our "optimum" DFT-TZVP basis set and used it to derive some of these molecular properties. These were compared with experimentally determined values, and those from other MO calculations, to see how well this "optimum" basis set was also able to reproduce cubane's molecular properties.

5.1. Molecular Geometries. In general, our calculations of molecular geometric properties using the TZVP basis set are in excellent agreement with experimentally determined molecular properties and compare favorably with the results from other MO calculations. The present results are summarized in Table 2. In particular, the carbon−carbon bond distance of 1.575 Å from our calculations agreed very well with the two most accurate experimentally determined values of 1.571 Å from electron diffraction[49] and microwave spectroscopic methods.[50] This compares with 1.551 Å from a lower accuracy X-ray diffraction study.[6] The carbon−hydrogen bond lengths were 1.098 Å from our TZVP calculations, compared with 1.097 Å by microwave spectroscopy,[50] 1.098 Å by electron diffraction,[49] 1.040 Å from the lower accuracy X-ray diffraction study, and the recommended value of 1.109 Å from Tsanaktsidis.[4] Our calculations yielded CCC bond angles of 90.00° and CCH bond angles of 125.25° also in excellent agreement with the electron diffraction[49] and microwave values. Miaskiewicz and Smith[15] recently published a theoretical study of cubane using the 6-31G* basis set and several DFT functionals. Their[15] geometries derived from the BPW91 functionals were similar to ours in terms of agreement with accurate microwave and electron diffraction geometries, with the other functionals yielding inferior results.

5.2. NMR Properties. Della et al.[12] measured the NMR spectra of cubane and derived the $^{13}C-H$ one-bond coupling constant. Their experimentally derived value of 153.8 Hz is in very good agreement with our theoretical values of 153.6−154.7 Hz, using the TZVP basis set and the IGLO method, and 154.1−155.0 Hz using the LORG method. Eaton and Cole[2] also measured the NMR spectra of cubane and obtained a value of 155 Hz for this coupling constant. Della and co-workers used an empirical relationship to derive a % s character of the carbon bonding orbital of 30.8%, in good agreement with the value of

(42) Brunger, M. J.; Braidwood, S. W.; McCarthy, I. E.; Weigold, E. *J. Phys. B* **1994**, *27*, 597.
(43) Jursic, B. S. *Theochem (J. Mol. Struct.)* **1997**, *394*, 15.
(44) Wang, H.; Law, C. K. *J. Phys. Chem. B* **1997**, *101*, 3400.
(45) Ball, D. W. *Theochem (J. Mol. Struct.)* **1996**, *364*, 183.
(46) Alkorta, I.; Elguero, *J. Tetrahedron* **1997**, *53*, 9741.
(47) Disch, R. L.; Schulman, J. M. *J. Am. Chem. Soc.* **1988**, *110*, 2102.
(48) Maksic, Z. B.; Randic, M. *J. Am. Chem. Soc.* **1973**, *95*, 6522.
(49) Almenningen, A.; Jonvic, T.; Martin, H. D.; Urbanek, T. *J. Mol. Struct.* **1985**, 128, 239.
(50) Hirota, E.; Fujitake, M.; Della, E. W.; Pigou, P. E.; Chickos, J. S. *J. Mol. Struct.* **1988**, *190*, 235.

Table 3. Calculated and Experimental (see Text) Vibrational Frequencies (cm^{-1}) of Cubane[a]

assignment[13]	expt IR[13]/Raman[14]	present TZVP	present TZVP (scaled)
C-C-C bend	617	553	582
C-C-C bend	667	623	656
C-C stretch	821	736	788
C-C stretch	829	783	838
C-C stretch	852	794	850
C-C stretch	899	821	879
C-C stretch	1001	970	1038
C-C-C bend	1030	1003	1056
C-C-H bend	1036	1022	1063
C-C-H bend	1078	1037	1078
C-C-H bend	1083	1040	1082
C-C-H bend	1130	1096	1140
C-C-H bend	1183	1121	1166
C-C-H bend	1235	1163	1210
C-H stretch	2965	3046	2966
C-H stretch	2972	3054	2974
C-H stretch	2990	3060	2981
C-H stretch	2994	3077	2997

[a] Assignment of cubane vibrational modes follows the work of Vlahacos et al.[13] The C−C−H bending mode can be alternatively described as C−H wagging.

31.1% determined at the MP2/6-31G** level of theory[4] and the value of 31% derived from $J^{13}{}_{C-H}$ NMR measurements of Eaton and Cole.[2]

5.3. Vibrational Spectra. There have been a number of experimental determinations of the vibrational spectrum of cubane, both infrared (IR) and Raman. Della and his colleagues first measured the solution (CS_2 and CCl_4) and solid-phase IR and Raman spectra.[14] More recently Pine et al.[51] have used a tunable laser to investigate the vibrational spectrum of cubane and derived a quadratic force field for the molecule.

There have also been several theoretical studies of the vibrational spectra of cubane and its isotropically substituted forms, using various levels of MO theory. Jursic[43] employed hybrid and gradient-corrected density functional theory methods to compute the IR and Raman spectra of cubane. He found that the B3LYP method gave the best agreement with experiment, especially after correcting the theoretical spectrum using empirical correlation factors to improve the agreement with experiment. Recently, Miaskiewicz and Smith[15] compared the performance of various DFT functionals with, and without, additional frequency scaling for calculating the cubane vibrational frequencies. They found that BPW91, BLYP, and B3LYP functionals gave good agreement with experimental spectra and also acceptable geometries for cubane, with the BPW91 functional being the best compromise. They noted that the SVWN functional, which is the "cheapest" of all DFT methods, gave very good spectral prediction, albeit with worse prediction of geometry.

Table 3 shows the vibrational frequencies calculated using DFT-TZVP from our work, compared with the experimentally measured infrared and Raman spectra of cubane. The calculated intensities of the transitions from our TZVP basis are also in reasonable agreement with the observed experimental IR spectrum of cubane,[14,51] as Table 4 illustrates. Our DFT-TZVP calculations gave frequencies of the vibrational modes of cubane in quite good agreement with experiment. After applying small empirical scaling factors (of C−C−C bend, 1.053; C−C stretch, 1.070; C−C−H bend, 1.040; C−H stretch, 0.974) to the frequencies, the predictions were considerably improved. Our scaling factors are similar to those derived by Miaskiewicz and Smith[15] and Jursic.[43] We note that the present calculations give results of comparable accuracy to those of Miaskiewicz and Smith.[15] The TZVP basis set is thus a good compromise where an accurate prediction of geometry and vibrational spectra is required.

Table 4. Calculated IR Intensities (km/mol) of Three IR-Active Modes of Cubane (O_h Symmetry)[a]

freq (cm^{-1}) (CS_2 soln[14])	IR band	qualitative experimental intensity	calcd IR intensity present TZVP
851	C-C stretch	strong	14.0
1228	C-C-H bend	strong	5.4
2977	C-H stretch	very strong	124

[a] The experimental data are the CS_2 solution measurements from Della et al.[14]

5.4. Electronic Properties. The molecular electrostatic potentials from our DFT-TZVP calculations are symmetric. In addition these calculations also indicated negative charge on the carbon atoms (Mulliken net atomic charge −0.116, Löwdin net atomic charge −0.101, charges fitted to electrostatic potential −0.032) and balancing positive charges on the hydrogen atoms.

We also investigated the electron density in the carbon−carbon region of cubane and found that the maximum electron density lies off the carbon−carbon axis by approximately 0.05 Å, consistent with the "bent bond" hypothesis for highly strained molecules. The off-axis electron density implies a bond angle of approximately 93.5°, i.e., the electron density in the bond forms an angle of approximately 3.5° with the carbon−carbon axis.

We also carried out a study analogous to that of Wiberg and colleagues,[52] to estimate the electron density (ρ) at the bond critical point (midway between the two carbons and at the center of maximum electron density off the carbon−carbon axis). We obtained a value of $\rho_b = 0.224 a_0^{-3}$. We then employed Wiberg's empirical method to calculate bond orders from electron densities at the bond critical points derived from the TZVP basis functions. The electron densities at the bond critical points of the model compounds ethane, ethene, ethyne, and benzene (bond orders of 1.0, 2.0, 3.0, and 1.5, respectively) were used to determine the constants in the relation between bond order n and the bond critical point densities ρ_b:

$$n = \exp\{7.075(\rho_b - 0.2377)\} \quad (5)$$

This relationship yielded a bond order for the carbon−carbon bonds in cubane of 0.91, a value in quite good accord with that found by Wiberg et al.[52] ($n = 0.95$) with their HF/6-31G* basis. We also calculated the bond order of the carbon−carbon bonds using Mulliken and Mayer populations analysis. The Mayer bond order of 0.95 was in reasonable agreement with our value. The Mulliken value of 0.58, on the other hand, reflects the well-known deficiencies of this method of orbital decomposition.

6. Conclusions

We have reported on the first comprehensive EMS study into the complete valence electronic structure of cubane. Momentum distributions for the $2t_{2g} + 1t_{2u}$, $1e_g$, $2t_{1u}$, $1a_{2u}$, $2a_{1g}$, $1t_{2g}$, $1t_{1u}$, and $1a_{1g}$ orbitals were measured and compared against an extensive series of PWIA-based calculations using DFT basis sets. Our calculations, for all seven basis sets constructed from the UniChem program,[28,29] were performed both at the LDA

(51) Pine, A. S.; Maki, A. G.; Robiette, A. G.; Krohn, B. J.; Watson, J. K. G.; Urbanek, T. *J. Am. Chem. Soc.* **1984**, *106*, 891.

(52) Wiberg, K. B.; Bader, R. F. W.; Lau, C. C. H. *J. Am. Chem. Soc.* **1987**, *109*, 985.

level and with the inclusion of BP and BLYP nonlocal correlation corrections to the DFT functional. On the basis of this comparison between the experimental and theoretical MDs, we found that the TZVP basis set provided the most physically reasonable representation of the cubane wave function. Molecular property information derived from our "optimum" TZVP basis was found to be in very good agreement with the available results from independent measurements. This result in cubane, when coupled with our earlier findings in [1.1.1]propellane,[53] butadiene,[54] and ethylene oxide,[55] firmly establishes the pedigree of EMS as a spectroscopic tool for a priori basis set evalution.

Future studies should now concentrate on larger molecular systems, which have become feasible with the improved energy resolution capability of the present EMS spectrometer, or on molecules such as norbornadiene where questions relating to some aspects of its bonding remain topical.[56] In addition, we note that an improvement in the reaction mechanism description, particularly for inner valence and core states, by the development of a distorted wave framework for multicentered targets, i.e., molecules, would be desirable.

Acknowledgment. We thank Drs. I. Lochert and A. Knill for their assistance with the synthesis of cubane. One of us (M.J.B.) also acknowledges the Australian Research Council for his Fellowship, and the Small Grant that provided financial support for this study. M.J.B. also thanks Dr. W. R. Newell and his colleagues for their hospitality during his visit to University College London. W.v.N. acknowledges the Fonds der Chemischen Industrie for partial support.

Supporting Information Available: Figures 5−9 depicting the 1000 eV symmetric noncoplanar momentum distributions for the $1e_g$, $2t_{1u}$, $1a_{2u}$, $1t_{2g}$, and $1t_{1u}$ orbitals of cubane (PDF). This material is available free of charge via the Internet at http://pubs.acs.org.

JA9940423

(53) Adcock, W.; Brunger, M. J.; Clark, C. I.; McCarthy, I. E.; Michalewicz, M. T.; von Niessen, W.; Weigold, E.; Winkler, D. A. *J. Am. Chem. Soc.* **1997**, *119*, 2896.

(54) Brunger, M. J.; Weigold, E.; Michalewicz, M. T.; Winkler, D. A. *J. Chem. Phys.* **1998**, *108*, 1859.

(55) Winkler, D. A.; Michalewicz, M. T.; Wang, F.; Brunger, M. J. *J. Phys. B* **1999**, *32*, 3239.

(56) Takahashi, M.; Ogino, R.; Udagawa, Y. *Chem. Phys. Lett.* **1998**, *288*, 714.